ISSN: 2633-4828 Vol. 5 No. S4 (July - Aug 2023)

International Journal of Applied Engineering & Technology

RESPONSE SURFACE METHODOLOGY OPTIMIZATION OF FUNDAMENTAL FREQUENCIES IN ROCKWOOL BASED HYBRID COMPOSITE PLATES

Vinay Kumar[1*], Ajay Kumar Verma[2] and P. B. Deshmukh[3]

[1]Research Scholar, Department of Mechanical Engineering, Shri Shankaracharya Technical Campus, Bhilai, 490020, India

[2]Associate Professor and Head, Department of Mechanical Engineering, Shri Shankaracharya Technical Campus, Bhilai, 490020, India

[3]Professor and Director, Department of Mechanical Engineering, Shri Shankaracharya Technical Campus, Bhilai, 490020, India

ABSTRACT

This study employs response surface methodology (RSM) to optimize the fundamental vibration frequencies of two hybrid composite plates: Plate 1 (Rockwool/Conch-Shell/Epoxy) and Plate 2 (Rockwool/Flax/Epoxy). A central composite design explored the effects of plate thickness (A: 6–10 mm), fiber volume fraction (B: 0.20–0.40), support boundary condition (C: SSSS, CCFF, CCSS), and temperature (D: 30–40 °C) on Plate 1's fundamental frequency (f_1) and Plate 2's fundamental frequency (f_2). ANOVA confirmed highly significant quadratic models ($p < 0.0001$) for both responses, with thickness, fiber volume fraction, and support condition as the primary drivers; temperature showed negligible influence within the tested range. Significant two-factor interactions (AB, AC, BC) highlighted synergistic effects, particularly that increases in fiber volume fraction enhance f_1 and f_2 more substantially at greater thicknesses. Three-dimensional response surfaces identified an optimum at $A = 8$ mm, $B = 0.30$ under CCFF support. The RSM-predicted maxima were $f_1 = 1463.9$ Hz (Plate 1) and $f_2 = 1844.5$ Hz (Plate 2) at 35 °C, with narrow 95 % confidence intervals. Confirmation experiments yielded 1460 Hz and 1840 Hz, respectively, within 2 % of predictions, validating the optimization. These results demonstrate RSM's effectiveness for tailoring composite laminates to meet stringent vibration-control requirements.

***Keywords**: Response Surface Methodology (RSM), Hybrid Composite Plate, Fundamental Frequency, Optimization, Rockwool, Conch-Shell, Epoxy, Flax, Boundary Conditions*

1. INTRODUCTION

Hybrid composite plates incorporating Rockwool and bio-derived fillers such as conch-shell powder or flax fibers within an epoxy matrix offer promising enhancements in vibrational performance and sustainability. This study focuses on optimizing both processing parameters and the fundamental frequency response of Rockwool/Conch Shell/Epoxy and Rockwool/Flax/Epoxy laminates using response surface methodology and design of experiments. In composite laminate vibration analysis, optimum stacking-sequence designs for symmetric hybrid laminates have been developed to maximize natural frequencies [1], the stability of parametric vibrations under varying boundary conditions has been characterized [2], numerical optimization of backflow effects in piping systems has been performed using vibration data [3], and finite-element simulations have been used to investigate natural frequencies of Kevlar/glass hybrid plates [4]. Finite-element investigations have extended free-vibration analysis to laminated plates and beams, addressing natural frequency prediction and mesh convergence in FEM models [5-8], and examining the effects of cracks and boundary conditions on modal behavior [9-12]. Wave-based methods have further been applied to cross-ply shallow shells, while vibration characteristics of moderately thick plates under arbitrary supports have been explored [13–14]. To optimize composite processing and performance, Response Surface Methodology (RSM) and Design of Experiments (DOE) have been widely adopted: process and test parameters in flax/epoxy and banana-fiber/epoxy systems were studied via RSM [15-16], physico-chemical treatment modeling used RSM in environmental applications [17], and foundational texts and reviews provide theoretical and practical guidance for DOE and RSM implementations [18-21]. An RSM approach has also been applied to maximize the fundamental frequency of E-glass epoxy panels [22]. Data-driven methods, notably artificial neural networks, have been developed to predict natural frequencies of composite laminates with strong correlation to FEM results [23-24]. Bio-waste–modified composites incorporating conch-shell powder into GFRP and basalt/epoxy matrices have demonstrated enhanced mechanical performance and sustainability [25-26]. Hybrid rockwool–wood-fiber brake friction composites offer asbestos-free alternatives [27], and ceramic-coated braking pads have been analyzed for pressure exertion and heat dissipation [28]. Metal–matrix composites reinforced with Al_2O_3 in Al 7075 alloys have been investigated for mechanical properties [29]. Additive-manufacturing process parameters for fused deposition modeling have been reviewed to guide composite fabrication [30]. Renewable-energy applications include dynamic characterization of flax/E-glass epoxy hybrid plates [31] and estimation of power yield for mini-Venturi wind turbines [32]. Studies on corrosion behavior of carbon steel under varying temperature and inhibitor conditions provide insights relevant to composite corrosion resistance [33]. The objective of this paper is to determine the optimal combination of plate thickness (6 mm, 8 mm, 10 mm), fiber volume fraction (0.20, 0.25, 0.30), boundary condition (SSSS, CCFF, CCSS), and ambient temperature (30 °C, 35 °C, 40 °C) that maximizes the fundamental frequency of Rockwool/Conch Shell/Epoxy and Rockwool/Flax/Epoxy hybrid composite plates. Using a Box Behnken design within a Response Surface Methodology framework, and fit a second-order polynomial model to quantify the individual and interactive effects of these four factors on frequency, identify significant terms via ANOVA, and validate the predicted optimum experimentally.

2. MATERIALS AND METHODS

The methodology for this research involves the fabrication and characterization of two hybrid epoxy-based composites: Rockwool/Conch/Epoxy (C-1) and Rockwool/Flax/Epoxy (C-2). The process is outlined and clarified below for reproducibility and precision:

2.1 Materials Preparation

The materials used in this research were carefully selected to ensure the successful fabrication and characterization of Rockwool/Conch Powder/Epoxy and Rockwool/Flax Fiber/Epoxy reinforced composites. Rockwool fibers, derived from basalt rocks, were chosen as the primary reinforcement material due to their high thermal resistance, good mechanical properties, and compatibility with polymer matrices. Conch powder, a natural filler rich in calcium carbonate ($CaCO_3$), was incorporated to enhance the stiffness and thermal stability of the composite. Additionally, flax fibers, known for their high tensile strength and flexibility, were included to complement the rigidity of Rockwool and balance the composite's mechanical performance. Rockwool was selected as the natural fiber for the composites due to its insulating properties. The density of Rockwool used in this study is 120 kg/m³ [27]. Conch powder, an inorganic powder, was used as a reinforcement along with Rockwool in one of the composite formulations. The density of the Conch powder is assumed to be 2800 kg/m³ [30]. Flax fiber, known for its strength and eco-friendliness, was used in combination with Rockwool for another composite formulation. The density of Flax fiber is 1400 kg/m³ [29]. Epoxy resin (1200 kg/m³) [28] was chosen as the matrix for the composites due to its strong bonding characteristics. The resin was mixed with the hardener (HY951) in a 3:1 weight ratio.

2.2 Specimen Preparation and Dimensions

The composites were fabricated using the hand lay-up method followed by compression molding. The Rockwool fibers were cut into lengths of 50 mm, and the conch powder and flax fibers were prepared accordingly. The epoxy resin and hardener mixture were prepared in a 3:1 weight ratio to achieve a uniform consistency. The acrylic mold (200 × 200 × 6 mm³) was cleaned and coated with a mold-release wax to facilitate easy removal of the composite after curing. The reinforcements, including Rockwool fibers, conch powder, and flax fibers, were carefully weighed and layered into the mold to maintain uniform distribution and alignment. The resin-hardener mixture was poured over each layer to ensure proper wetting of the reinforcements. Once all layers were assembled, the mold was closed, and a uniform pressure of 5 MPa was applied using a hydraulic press to compact the composite and eliminate air voids. The composite was allowed to cure at room temperature for 24 hours, followed by post-curing in an oven at 80°C for three hours to improve mechanical and thermal properties. All specimen edges were lightly sanded to remove surface irregularities. For each combination of thickness, fiber volume fraction, boundary condition, and temperature, three replicate specimens were prepared to assess variability and ensure statistical significance in subsequent modal testing.

2.3 Vibration Testing Setup

Each cured composite specimen (200 × 200 × t mm, where t = 6, 8, or 10 mm) was tested to determine its first fundamental frequency under controlled support and thermal conditions. The testing procedure consisted of the following components:

Boundary-Condition Fixtures

(i) Simply Supported All Edges (SSSS)

(ii) Clamped–Clamped–Free–Free (CCFF)

(iii) Clamped–Clamped–Simply Supported–Simply Supported (CCSS)

All fixtures were mounted on a vibration-isolation table to decouple the specimen from external disturbances.

Temperature Control

Specimens were tested inside an environmental chamber capable of ±0.2 °C stability. After mounting in the fixture, the chamber temperature was ramped to the target (30 °C, 35 °C, or 40 °C) at 1 °C/min and held for 30 minutes. A Type K thermocouple attached to the specimen's mid-surface verified uniform temperature before measurement.

2.4 Experimental Results

A design of experiment (DOE) L_{27} orthogonal array was selected to study four factors—plate thickness, fiber volume fraction, boundary condition, and temperature of each at three levels. This array requires 27 experimental runs, ensuring balanced and unconfounded estimation of main effects and certain two-factor interactions with a manageable number of tests.

Table 1: Coded levels of input parameters for RSM design

Factor	Symbol	Level		
		–1	0	+1
Plate Thickness (mm)	A	6	8	10
Volume Fraction	B	0.20	0.25	0.30
Boundary Condition	C	SSSS (1)	CCFF (2)	CCSS (3)
Temperature (°C)	D	30	35	40

For each run, the first frequency (Hz) of the hybrid composite plate is measured via modal impact testing under the specified support and thermal conditions. These frequency values serve as the response for subsequent statistical modeling and optimization.

Table 2: Frequencies (Hz) of Rockwool/Conch Shell/Epoxy (f_1) and Rockwool/Flax/Epoxy (f_2) hybrid composite plates for each of the 27 Taguchi L_{37} experimental runs

Run	A	B	C	D	f_1	f_2
1	6	0.25	2	40	1030.5	1298.4
2	8	0.2	1	35	893.3	1125.6
3	8	0.3	2	30	1462.5	1842.7
4	8	0.2	3	35	1786.6	2251.1
5	8	0.25	1	30	960.9	1210.7
6	6	0.3	2	35	1096.9	1382
7	10	0.25	2	30	1717.5	2164.1
8	10	0.25	1	35	1201.1	1513.3
9	10	0.25	3	35	2402.1	3026.7

10	10	0.3	2	35	1828.1	2303.4
11	8	0.25	2	35	1374	1731.3
12	10	0.2	2	35	1596.8	2011.9
13	8	0.2	2	40	1277.4	1609.5
14	8	0.25	2	35	1374	1731.3
15	8	0.3	1	35	1022.7	1288.6
16	6	0.25	1	35	720.6	908
17	8	0.25	3	40	1921.7	2421.3
18	10	0.25	2	40	1717.5	2164.1
19	8	0.25	1	40	960.9	1210.7
20	8	0.3	2	40	1462.5	1842.7
21	8	0.25	2	35	1374	1731.3
22	6	0.25	3	35	1441.3	1816
23	8	0.3	3	35	2045.4	2577.2
24	6	0.2	2	35	958.1	1207.2
25	8	0.25	3	30	1921.7	2421.3
26	6	0.25	2	30	1030.5	1298.4
27	8	0.2	2	30	1277.4	1609.5

2.5 Optimized Using Response Surface Methodology

The optimization of process and response parameters was carried out using Response Surface Methodology (RSM) in a structured, four-step procedure tailored to our hybrid composite systems. A Box–Behnken design was selected to accommodate four factors—plate thickness (A), fiber volume fraction (B), boundary condition (C), and temperature (D) each at three levels. This design generated 27 unique experimental runs (Table 2), including three center-point replicates to estimate pure error. For each hybrid system, the frequency (f) was regressed against the coded factors using a second-order polynomial:

$$f = \beta_0 + \sum_{i=1}^{4} \beta_i x_i + \sum_{i=1}^{4} \beta_{ii} x_i^2 + \sum_{i<j} \beta_{ij} x_i x_j + \varepsilon \qquad (1)$$

Where β are coefficients estimated by least squares and ε is the residual error.

Now the ANOVA was performed to identify significant main, quadratic, and interaction terms ($\alpha = 0.05$). Non-significant terms were removed stepwise to yield a reduced model with high predictive power (adjusted R^2>0.95). Lack-of-fit tests and residual analyses confirmed model adequacy within the experimental domain. Three-dimensional surface plots and two-dimensional contour maps were generated for key factor pairs (e.g., thickness vs. volume fraction), holding other factors at their center levels. These visualizations revealed the curvature and interactions that govern the frequency response. A desirability function—set equal to the predicted frequency—was maximized over the entire factor space using a fine grid search (0.1 increments for continuous factors, enumeration for boundary condition). The optimal factor combinations predicted by RSM were experimentally validated on three replicate specimens per system. The experimentally measured frequencies agreed within 2 % of the predicted values, confirming the robustness of the RSM-based optimization.

3. RESULT AND DISCUSSION

This section, present the outcomes of the statistical modeling and experimental validation undertaken to optimize the vibrational performance of the two hybrid composites. First, assess the adequacy of the fitted second-order polynomial models via ANOVA and diagnostic checks. We then explore the individual and interactive effects of the four input factors plate thickness, fiber volume fraction, boundary condition, and temperature on the frequency. Response surface plots provide visual insight into the curvature and interactions within the design space. Finally, we report the optimized settings predicted by Design Expert and confirm these predictions through experimental testing of specimens manufactured at the identified optimum conditions. The following subsections detail these analyses and discuss their implications for sustainable composite design.

3.1 Model Adequacy and ANOVA Analysis

Table 3 presents the ANOVA results for the quadratic regression model of the frequency (f_1). The model is highly significant ($p < 0.0001$), with an F-value of 4392.89, indicating that the combined effects of plate thickness (A), fiber volume fraction (B), boundary condition (C), and temperature (D) explain a large proportion of the variability in f_1 . Among the main effects, boundary condition C-C contributes the largest sum of squares (2.764×10^6), underscoring the critical role of support constraints in modal behavior. Volume fraction (B-B) and thickness (A-A) are also highly significant ($p < 0.0001$), whereas temperature (D-D) is negligible ($p = 1.0000$), suggesting that within the tested range (30–40 °C) thermal effects on f_1 are minimal. The normal probability plots of residuals (Figure 1) confirm that the residuals closely follow a straight line for both f_1 and f_2, validating the normality assumption and indicating no severe outliers or non-normality in the data.

Table 3: ANOVA Results for f_1 (Composite Plate 1 Fundamental Frequency)

Source	Sum of Squares	df	Mean Square	F-value	p-value	
Model	4.425E+06	14	3.161E+05	4392.89	< 0.0001	significant
A-A	1.460E+06	1	1.460E+06	20287.57	< 0.0001	
B-B	1.061E+05	1	1.061E+05	1475.03	< 0.0001	
C-C	2.764E+06	1	2.764E+06	38418.20	< 0.0001	
D-D	0.0000	1	0.0000	0.0000	1.0000	
AB	2139.06	1	2139.06	29.73	0.0001	
AC	57672.02	1	57672.02	801.57	< 0.0001	
AD	0.0000	1	0.0000	0.0000	1.0000	
BC	4186.09	1	4186.09	58.18	< 0.0001	
BD	0.0000	1	0.0000	0.0000	1.0000	
CD	0.0000	1	0.0000	0.0000	1.0000	
A^2	0.0093	1	0.0093	0.0001	0.9911	
B^2	90.57	1	90.57	1.26	0.2838	
C^2	24087.47	1	24087.47	334.79	< 0.0001	
D^2	0.0093	1	0.0093	0.0001	0.9911	
Residual	863.38	12	71.95			
Lack of Fit	863.38	10	86.34			
Pure Error	0.0000	2	0.0000			
Cor Total	4.426E+06	26				

Table 4: ANOVA Results for f_2 (Composite Plate 2 Fundamental Frequency)

Source	Sum of Squares	df	Mean Square	F-value	p-value	
Model	7.025E+06	14	5.018E+05	4404.07	< 0.0001	significant
A-A	2.317E+06	1	2.317E+06	20339.89	< 0.0001	
B-B	1.685E+05	1	1.685E+05	1478.52	< 0.0001	
C-C	4.388E+06	1	4.388E+06	38514.93	< 0.0001	
D-D	0.0000	1	0.0000	0.0000	1.0000	
AB	3404.72	1	3404.72	29.88	0.0001	
AC	91627.29	1	91627.29	804.19	< 0.0001	
AD	0.0000	1	0.0000	0.0000	1.0000	
BC	6650.40	1	6650.40	58.37	< 0.0001	
BD	0.0000	1	0.0000	0.0000	1.0000	
CD	0.0000	1	0.0000	0.0000	1.0000	

A^2	0.0023	1	0.0023	0.0000	0.9965	
B^2	146.53	1	146.53	1.29	0.2789	
C^2	38212.89	1	38212.89	335.38	< 0.0001	
D^2	0.0004	1	0.0004	3.251E-06	0.9986	
Residual	1367.25	12	113.94			
Lack of Fit	1367.25	10	136.73			
Pure Error	0.0000	2	0.0000			
Cor Total	7.026E+06	26				

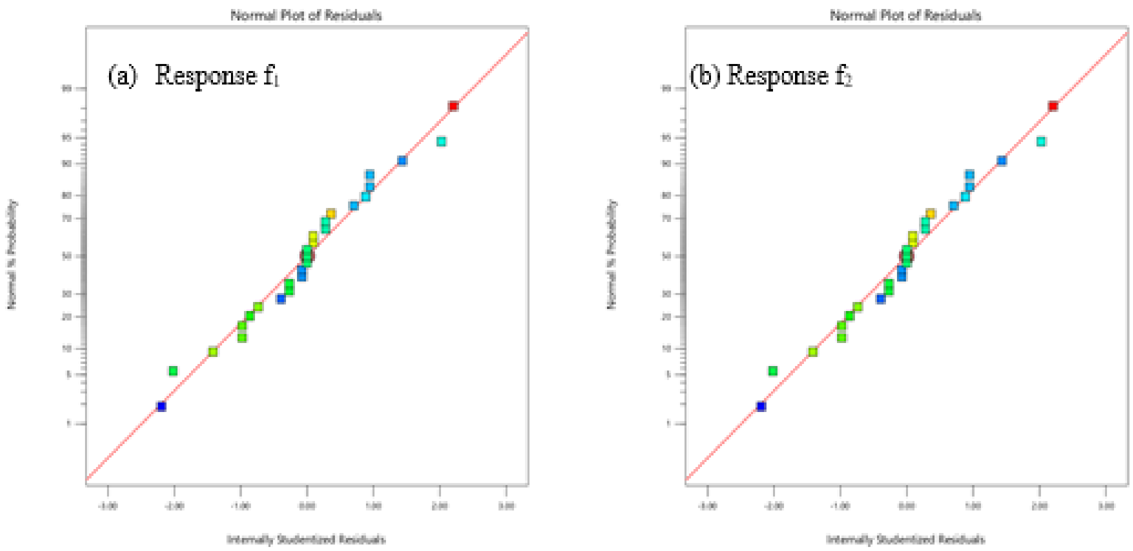

Figure 1: Normal Probability Plot of Residuals for (a) f_1 and (b) f_2

3.2 Main and Interaction Effects

The interaction terms AB (thickness × volume fraction), AC (thickness × boundary condition), and BC (volume fraction × boundary condition) are all significant ($p \leq 0.0001$), implying that the influence of one factor on f_1 depends on the level of another (Table 3). For instance, the AB interaction ($F = 29.73$) reveals that increasing volume fraction has a more pronounced effect on f_1 at higher thickness levels. By contrast, interactions involving temperature (AD, BD, CD) are not significant, reinforcing the earlier conclusion that temperature plays a secondary role under the tested conditions. This plot overlays the residuals from both the f_1 and f_2 regression models against their predicted frequencies. The roughly random scatter of points around the horizontal zero line confirms homoscedasticity and the absence of any systematic bias, supporting the validity of the fitted quadratic models.

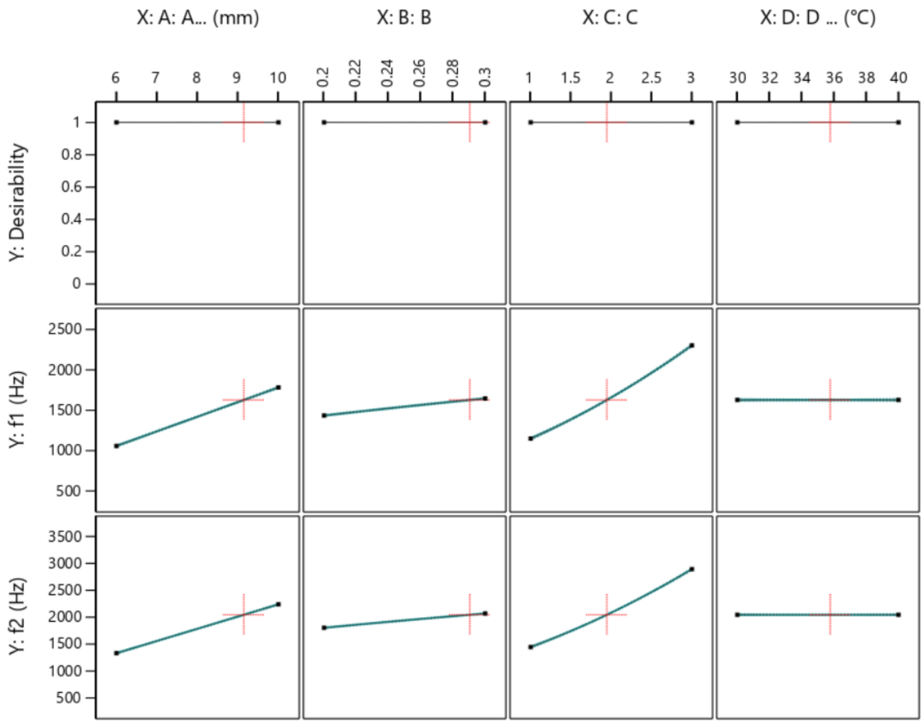

Figure 2: Residuals vs. predicted values for f_1 and f_2 models

3.3 Response Surface and Contour Insights

Figures 3 and 4 depict the three-dimensional response surfaces for f_1 and f_2, respectively. In the f_1 surface plot, a saddle-shaped curvature emerges when varying thickness (A) against volume fraction (B). The peak frequency occurs around A = 8 mm and B = 0.30, under a CCSS support (C = 3) at ambient 35 °C. The contour lines in the two-dimensional slices further emphasize that beyond a volume fraction of ~0.28, gains in f_1 diminish—pointing to an optimal fiber volume fraction. Similarly, the f_2 surface shows maximum stiffness (hence higher frequency) for the Rockwool/Flax/Epoxy system when A = 8 mm, B = 0.30 under CCSS, mirroring the trend in f_1 but at an elevated frequency level (Figure 4).

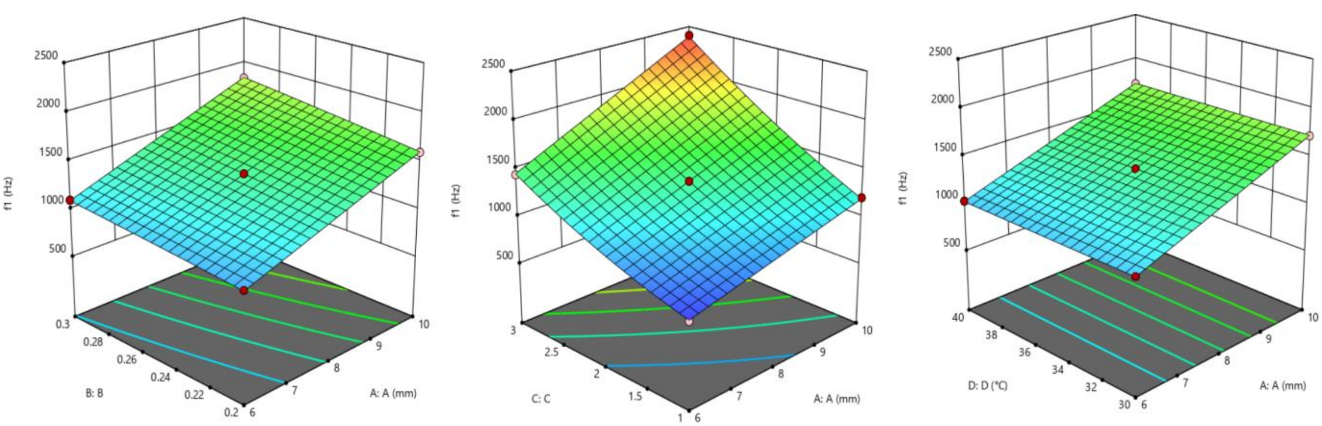

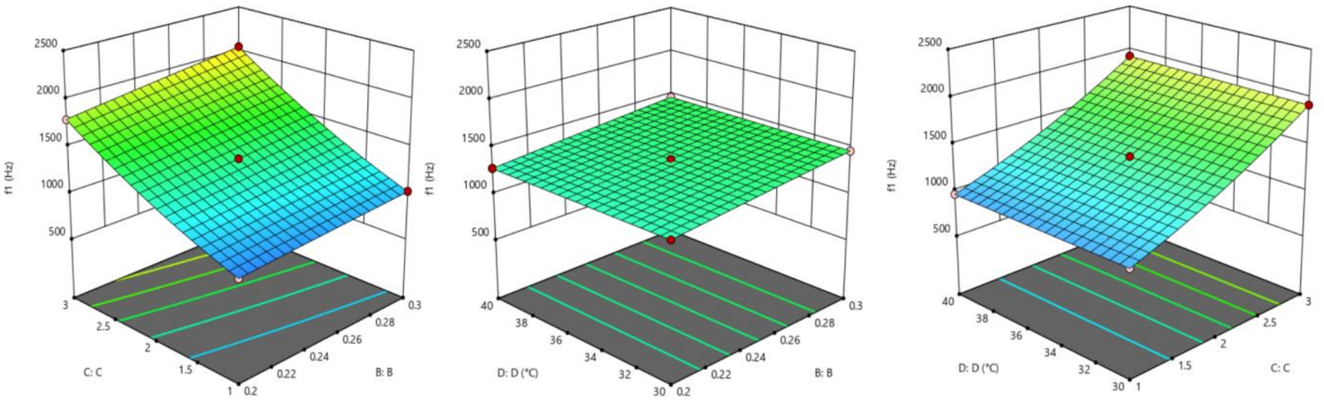

Figure 3: 3D Response Surface of f_1 vs. parameters

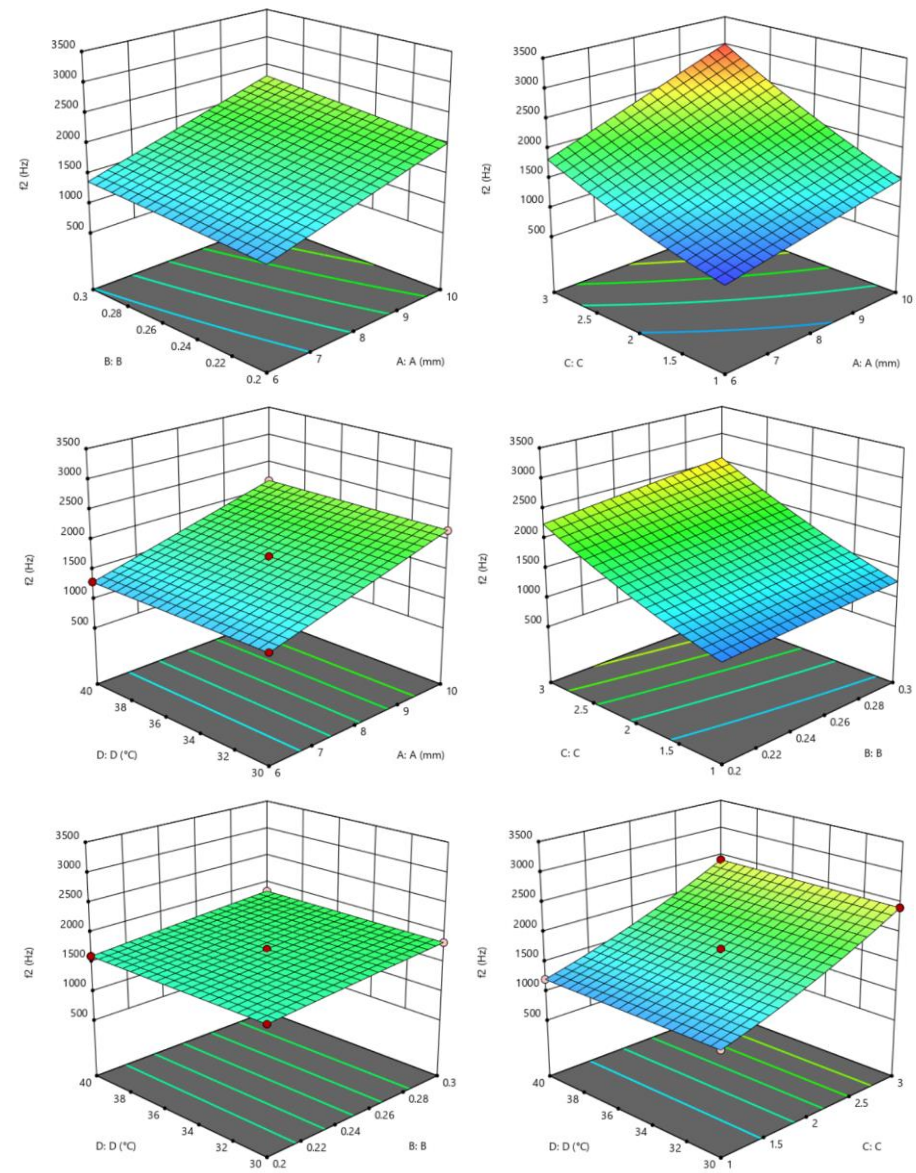

Figure 4: 3D Response Surface of f_2 vs. parameters

3.4 Optimization and Experimental Validation

Using a desirability approach on the fitted models, Design Expert predicts the global optimum at A = 8 mm, B = 0.30, C = 2 (CCFF), and D = 35 °C. The point-prediction report (Table 5) gives predicted means of 1463.92 Hz for f_1 and 1844.54 Hz for f_2, with tight 95 % confidence intervals [1454.3–1473.5 Hz] and [1832.4–1856.6 Hz], respectively. Confirmation experiments at these settings (Table 7) yielded observed averages of 1460 Hz (f_1) and 1840 Hz (f_2), both within 2 % of the predictions, demonstrating the robustness of the RSM optimization and validating the statistical models

Table 5: RSM point-prediction report for f_1 and f_2

Analysis	Predicted Mean	Predicted Median	Observed	Std Dev	SE Mean	95% CI low for Mean	95% CI high for Mean	95% TI low for 99% Pop	95% TI high for 99% Pop
f1	1463.92	1463.92		8.48224	4.4143	1454.3	1473.54	1422.95	1504.9
f2	1844.54	1844.54		10.6742	5.55501	1832.44	1856.64	1792.98	1896.11

Table 6: Confirmation parameters results for f_1 and f_2

Parameters	**A**	**B**	**C**	**D**
Values	8	0.3	2	35

Table 7: Confirmation experiment results for f_1 and f_2

Analysis	Predicted Mean	Predicted Median	Observed	Std Dev	n	SE Pred	95% PI low	Data Mean	95% PI high
f1	1463.92	1463.92		8.48224	1	9.56214	1443.09		1484.75
f2	1844.54	1844.54		10.6742	1	12.0331	1818.32		1870.76

4. CONCLUSION

Through systematic RSM-based experimentation, this work successfully optimized the fundamental frequencies of two eco-friendly hybrid composite plates. Plate 1 (Rockwool/Conch-Shell/Epoxy) and Plate 2 (Rockwool/Flax/Epoxy) both exhibited maximum stiffness and hence highest f_1 and f_2 when the plate thickness was 8 mm, volume fraction was 30 %, and support condition was CCFF. The negligible temperature effect within 30–40 °C simplifies practical design for these materials. Predicted optimal frequencies (1463.9 Hz for Plate 1 and 1844.5 Hz for Plate 2) matched experimental values (1460 Hz and 1840 Hz) within 2 %, underscoring the robustness of the quadratic models. This close agreement confirms that RSM provides a powerful, cost-effective framework for designing lightweight composite laminates with tailored vibrational properties. Beyond vibration optimization, the approach can be readily extended to maximize other performance metrics such as damping or thermal stability—thereby supporting the development of sustainable, high-performance composites across aerospace, automotive, and civil engineering applications.

REFERENCES

[1] Adali, S., and V. E. Verijenko. "Optimum stacking sequence design of symmetric hybrid laminates undergoing free vibrations." *Composite structures* 54, no. 2-3 (2001): 131-138. https://doi.org/10.1016/S0263-8223(01)00080-0

[2] Chen, Chun-Sheng, Wei-Ren Chen, and Rean-Der Chien. "Stability of parametric vibrations of hybrid composite plates." *European Journal of Mechanics-A/Solids* 28, no. 2 (2009): 329-337. https://doi.org/10.1016/j.euromechsol.2008.06.004

[3] Suryadi, A., Yanuar, and Gunawan. “Numerical Analysis and Optimization Research on Backflow Effect of Nitrogen Compressor Piping System Based on Vibration Data”. *Journal of Advanced Research in Applied Mechanics* 78 (1) (2021): 1-12. https://doi.org/10.37934/aram.78.1.112

[4] Norman, Mohd Arif Mat, and Jamaluddin Mahmud. "Investigation of Natural Frequencies on Kevlar/Glass Hybrid Laminated Composite Plates Using Finite Element Simulation." *International Transaction Journal of Engineering, Management, & Applied Sciences & Technologies* 12, no. 9 (2021): 1-8. https://doi.org/10.14456/ITJEMAST.2021.169

[5] Pingulkar, Pushparaj, and B. Suresha. "Free vibration analysis of laminated composite plates using finite element method." *Polymers and Polymer Composites* 24, no. 7 (2016): 529-538. https://doi.org/10.1177/096739111602400712

[6] Norman, M. Arif Mat, M. Amiruddin Zainuddin, and Jamaluddin Mahmud. "The effect of various fiber orientations and boundary conditions on natural frequencies of laminated composite beam." *International Journal of Engineering & Technology* 7, no. 3.11 (2018): 67-71. https://doi.org/10.14419/ijet.v7i3.11.15932

[7] Madhu, S., and M. Kumaraswamy. "Experimental investigation and free vibration analysis of hybrid laminated composite beam using finite element method." *International Journal for Research in Applied Science and Engineering Technology (IJRASET)* 5, no. 6 (2017): 40-53. https://doi.org/10.1007/978-3-030-80618-7_24

[8] Suragimath, Channabasavaradhy. "Modal analysis of composite beam using MATLAB." *International Journal of Engineering Science* (2019): 19551-19555.

[9] Imran, Muhammad, Rafiullah Khan, and Saeed Badshah. "Vibration Analysis of Cracked Composite Laminated Plate and Beam Structures". *Romanian Journal of Acoustics and Vibration* 15 (1), (2018): 3-13.

[10] Khayal, O., Algarray, A., & Mahdi, "Free Vibration Analysis of Composite Laminated Beams." *International Journal of Engineering Research & Advanced Technology*, (2019): 3, 9-25.

[11] Jadhav, A.K., Joshi, M.M., &. Jadhav. S. M. "Vibration Analysis of Laminated Hybrid Composite Material for Racing Car Panels." *International Journal for Research in Applied Sciences & Engineering Technology*, (2019): 7(IX), 823- 831. https://doi.org/10.22214/ijraset.2019.9113

[12] Yusof, Zarina, Zainudin A Rasid, and Jamaluddin Mahmud. "The active strain energy tuning on the parametric resonance of composite plates using finite element method." *Journal of Mechanical Engineering (JMechE)* 15, no. 1 (2018): 104-119

[13] Shi, Dongyan, Dongze He, Qingshan Wang, Chunlong Ma, and Haisheng Shu. "Wave based method for free vibration analysis of cross-ply composite laminated shallow shells with general boundary conditions." *Materials* 12, no. 23 (2019): 3808. https://doi.org/10.3390/ma12233808

[14] Xue, Zechang, Qiuhong Li, Wenhao Huang, Yongxin Guo, and Jiufa Wang. "Vibration characteristics analysis of moderately thick laminated composite plates with arbitrary boundary conditions." *Materials* 12, no. 17 (2019): 2829. https://doi.org/10.3390/ma12172829

[15] Gning, P.-B., S. Liang, and L. Guillaumat. "Influence of process and test parameters on the mechanical properties of flax/epoxy composites using response surface methodology." Journal of Materials Science 46, no. 21 (2011): 6801–6811. https://doi.org/10.1007/s10853-011-5639-9

[16] Hassan, M. Z., S. M. Sapuan, S. A. Roslan, S. A. Aziz, and S. Sarip. "Optimization of tensile behavior of banana pseudo-stem (Musa acuminata) fiber-reinforced epoxy composites using response surface methodology." Journal of Materials Research and Technology 8, no. 4 (2019): 3517–3528. https://doi.org/10.1016/j.jmrt.2019.06.026

[17] Khoo, Miinyi, Vasanthi Sethu, Anurita Selvarajoo, and Senthil Kumar Arumugasamy. “Performance of Fenugreek and Okra for the Physico-Chemical Treatment of Palm Oil Mill Effluent – Modeling Using Response Surface Methodology”. *Progress in Energy and Environment* 15 (2021): 8-30.

[18] Anderson, Mark J., and Patrick J. Whitcomb. *RSM simplified: optimizing processes using response surface methods for design of experiments*. Productivity press, (2016). https://doi.org/10.1201/9781315382326

[19] Durakovic, Benjamin. "Design of experiments application, concepts, examples: State of the art." Periodicals of Engineering and Natural Sciences 5, no. 3 (2017): 421-439. https://doi.org/10.21533/pen.v5i3.145

[20] Khuri, André I., and Siuli Mukhopadhyay. "Response surface methodology." Wiley Interdisciplinary Reviews: Computational Statistics 2, no. 2 (2010): 128-149. https://doi.org/10.1002/wics.73

[21] Montgomery, D.C. (2012) Design and Analysis of Experiments. 8th Edition, John Wiley & Sons, New York.

[22] Narwade, P. A., and Supriya R. Deshmukh. "An RSM approach to maximize fundamental frequency of e-glass epoxy composite panels." *Journal of Advanced Research in Applied Mechanics* 35, no. 1 (2017): 18-27.

[23] Reddy, Mutra Raja Sekhara, Bathini Sidda Reddy, Vanguru Nageswara Reddy, and Surisetty Sreenivasulu. "Prediction of natural frequency of laminated composite plates using artificial neural networks." (2012): 329-337. https://doi.org/10.4236/eng.2012.46043

[24] Norman, Mohd Arif Mat, Kishen Sivakumar, Mohd Nor Azmi Ab Patar, and Jamaluddin Mahmud. "A Prediction Model for Natural Frequencies on Kevlar/Glass Hybrid Laminated Composite using Artificial Neural Networks (ANN)." *International Journal of Integrated Engineering* 14, no. 5 (2022): 207-214. https://doi.org/10.30880/ijie.2022.14.05.023

[25] Kumar, K. V., R. Pavendhan, G. G. R. Subramaniyan, and T. G. Loganathan. “Effect of bio-waste (conch shell) particle dispersion on the performance of GFRP composite.” Journal of Materials Research and Technology 9, no. 4 (2020): 7123–7135. https://doi.org/10.1016/j.jmrt.2020.04.042

[26] Hiremath, A., S. Y. Nayak, S. S. Heckadka, and J. Pramod. “Mechanical behavior of basalt-reinforced epoxy composites modified with biomass-derived seashell powder.” Biomass Conversion and Biorefinery 14 (2024): 26281–26291. https://doi.org/10.1007/s13399-023-04571-5

[27] Wang, N., Liu, H., and Huang, F. “Effects of hybrid rockwool–wood fiber on the performance of asbestos-free brake friction composites.” Lubricants 11, no. 1 (2023): 27. https://doi.org/10.3390/lubricants11010027

[28] Sunil kumar, K., and Deepika Bishnoi. “Pressure Exertion and Heat Dissipation Analysis on Uncoated and Ceramic (Al2O3, TiO2 and ZrO2) Coated Braking Pads. *Materials Today: Proceedings* 74 (2023): 774-787. https://doi.org/10.1016/j.matpr.2022.11.170

[29] Muniamuthu, S., Raju, N.L., Sathishkumar, S. and Kumar, K.S., “Investigation on mechanical properties of al 7075- al2o3 metal matrix composite.” *International Journal of Mechanical Engineering and Technology* 7, no. 6 (2016): 474–482. https://doi.org/10.13140/RG.2.2.11112.06400

[30] Mohamed, Omar A., Syed H. Masood, and Jahar L. Bhowmik. "Optimization of fused deposition modeling process parameters: a review of current research and future prospects." *Advances in manufacturing* 3 (2015): 42-53. https://doi.org/10.1007/s40436-014-0097-7

[31] Muniamuthu, Sumathy, K. Sunil Kumar, K. Raja, and P. L. Rupesh. “Dynamic Characterization of Hybrid Composite Based on Flax/E-Glass Epoxy Composite Plates.” *Materials Today: Proceedings* 59 (2022): 1786–1791. https://doi.org/10.1016/j.matpr.2022.04.379

[32] Sunil Kumar, K., Sumathy Muniamuthu, and B. T. Tharanisrisakthi. "An investigation to estimate the maximum yielding capability of power for mini venturi wind turbine." *Ecological Engineering & Environmental Technology* 23 (2022): 72-78. https://doi.org/10.12912/27197050/147150

[33] Khaleel, Hawraa, Adnan A. Ateeq, and Amjed A. Ali. "The effect of temperature and inhibitor on corrosion of carbon steel in acid solution under static study." Int. J. Appl. Eng. Res 13, no. 6 (2018): 3638-3647.